Altered TNSALP Expression and Phosphate Regulation Contribute to Reduced Mineralization in Mice Lacking Androgen Receptor[▽][†]

Hong-Yo Kang,[1,2] Chih-Rong Shyr,[1,3] Chiung-Kuei Huang,[1] Meng-Yin Tsai,[1,4] Hideo Orimo,[5]
Pei-Chun Lin,[1] Chawnshang Chang,[6]* and Ko-En Huang[1,4]*

Center for Menopause and Reproductive Medicine Research[1] and Graduate Institute of Clinical Medical Sciences,[2] Chang Gung University and Chang Gung Memorial Hospital, Kaohsiung Medical Center, Kaohsiung, Taiwan; Department of Laboratory Medicine and Biotechnology, Tzu Chi University, Hualien, Taiwan[3]; Department of Obstetrics and Gynecology, Chang Gung University and Chang Gung Memorial Hospital, Kaohsiung Medical Center, Kaohsiung, Taiwan[4]; Division of Molecular Genetics and Nutrition, Department of Biochemistry and Molecular Biology, Nippon Medical School, Tokyo, Japan[5]; and George Whipple Lab for Cancer Research, Departments of Pathology and Urology, University of Rochester Medical Center, Rochester, New York[6]

While androgen receptor (AR)-deficient mice developed osteopenia in endochondral bones due to the high bone turnover with increased bone resorption by osteoclasts, little is known about the mechanism of intramembranous bone loss contributed by AR in osteoblasts. Here, we discovered a dramatic decrease in the area of calcification, new bone, and the number of osteocytes in calvaria from AR-deficient mice related to a reduction in mineralization caused, in part, by the diminished activity of AR-deficient osteoblasts. Enforced AR expression in differentiated osteoblasts boosts mineralization while knockdown of AR expression prevents androgen-induced mineralization. We identified the tissue-nonspecific alkaline phosphatase (TNSALP) and several members of small integrin binding ligand N-linked glycoprotein (SIBLING) gene family as androgen target genes required for AR-mediated bone formation. We show that inorganic phosphate (P_i) levels and TNSALP activity increased in response to androgen/AR and P_i signals increase the expression and translocation of AR. The ectopic expression of TNSALP or P_i partially rescued the bone loss due to AR deficiency. Thus, androgen/AR signaling plays an essential role in bone formation by coordinating the expression of genes associated with phosphate regulation.

The discovery of the central role of sex hormone deficiency in bone loss by Fuller Albright in 1947 provided the basis for elucidation of the mechanisms underlying the action of sex hormones on the skeleton, leading to significant improvements in the clinical management of patients with osteoporosis over the last few decades (12, 44). Clinical studies show that the combined therapy of estrogens with androgens in postmenopausal women enhances bone mineral density and bone mass more than estrogen therapy alone (5). Administration of flutamide, an androgen receptor (AR) antagonist, to rats results in osteopenia (15), thereby suggesting that androgen/AR signals may have a physiologically significant role in bone remodeling (32, 52).

Like the well-described target tissues for androgens, AR is widely distributed in bone, including osteoblasts, osteoclasts (20, 33, 42), and osteocytes (1). AR mRNA is upregulated by androgens in human osteoblastic cells in vitro (7, 48, 57, 58).

This increase in AR mRNA, coupled with the stabilization of AR protein after ligand binding, may enhance the ability of osteoblastic cells to respond to androgens. Our previous studies demonstrate that the stimulation of osteoblast proliferation by 5α-dihydrotestosterone (DHT) is blocked by AR antagonists and small interfering RNA (siRNA) (24). This finding supports the hypothesis that the effects of androgens on bone are mediated, at least in part, through AR in osteoblasts. Although androgens are believed to enhance osteoblast differentiation, improve the synthesis of extracellular matrix proteins, and stimulate mineralization through the AR, the molecular mechanisms underlying the regulation of bone matrix production and stimulating bone mineralization by androgens and the AR have not been well investigated.

Tissue-nonspecific alkaline phosphatase (TNSALP), encoded by the *AKP2* gene, is a membrane-bound phospho-ester phosphatase localized to the surface of osteoblasts. Mice in which the Akp2 gene has been inactivated mimic the form of hypophosphatasia, a disease characterized by rickets, osteomalacia, and spontaneous bone fractures with poor mineralization in the parietal bones, scapulae, vertebral bones, and ribs (10, 18, 19, 54, 55). Changes in the level of TNSALP protein have a significant effect on osteoblast and osteocyte function and consequent matrix mineralization, thereby indicating that TNSALP has key biological roles in the mineralization of bone (19). The specific mechanisms involved in regulating TNSALP function during bone formation are largely unknown.

Several reports show that global androgen receptor knockout (ARKO; AR[−/Y]) male mice develop osteopenia, resulting in definitive bone loss in conjunction with changes in histolog-

* Corresponding author. Mailing address for Ko-En Huang: Center for Menopause and Reproductive Medicine Research, Chang Gung University and Chang Gung Memorial Hospital, 12F, No. 123, Ta Pei Rd., Niao Sung Hsiang, Kaohsiung 833, Taiwan. Phone: (886) 7731-7123, ext. 2000. Fax: (886) 7733-6970. E-mail: khuang@adm.cgmh.org. Mailing address for Chawnshang Chang: George Whipple Lab for Cancer Research, Department of Pathology and Urology, University of Rochester Medical Center, 601 Elmwood Ave., Box 626, Rochester, NY 14642. Phone: (585) 275-9994. Fax: (585) 756-4133. E-mail: chang @urmc.rochester.edu.

ical analysis of tibia and femur bone sections (31, 53, 60). Trabecular and cortical bone mass are lower in ARKO mice than in both female and male wild-type littermates (46). A similar pattern of trabecular bone loss is also observed in male mice in which exon 3 of the AR gene is deleted specifically in mature osteoblasts (38). In vivo studies with transgenic mice overexpressing AR in osteoblastic cells confirm an important role for AR in bone formation and maintenance in males (59). Bone loss is the outcome of imbalanced bone resorption relative to bone formation (49). Although an imbalance of bone remodeling in endochondral bones caused by excessive osteoclast activity contributes to the pathogenesis of osteopenia in ARKO mice (31), our knowledge of androgen/AR actions on intramembranous bone formation by osteoblasts is limited. Our present studies reveal that ARKO mice have an impaired response to androgens in neonatal calvarial bones that exhibit a dramatic decrease in the area of calcification and suture width due to the diminished activity of AR-deficient osteoblasts. At the molecular level, the androgen and phosphate signaling pathways converge at the AR. Phosphate signals increase the expression and activity of AR, while phosphate levels and alkaline phosphatase (ALP) activity increase in response to androgen/AR signaling. Taken together, our results indicate that androgen/AR signaling controls an integrated gene expression program required for bone formation and mineralization.

MATERIALS AND METHODS

Animals. All animal procedures followed the *Guide for the Care and Use of Laboratory Animals* as promulgated by the Institute of Laboratory Animal Resources, National Research Council, National Academy of Science (United States), and were approved by the Animal Care and Use Committee of the Chang Gung Memorial Hospital at Kaohsiung Medical Center. Construction of targeting vectors and generation of the chimera founder mice have been described previously (60). The strains of the mosaic founder mice were C57BL/6 and 129Sv background. β-Actin is encoded by a housekeeping gene and is universally expressed in every tissue; therefore, the β-actin promoter-driven Cre (ACTB-Cre; Jackson Laboratories, Bar Harbor, ME) expresses and deletes floxed AR fragments in all of the tissues. The ARKO mice were genotyped by PCR as described previously (60). Animals were housed in pathogen-free facilities, maintained on a 12-h light/dark schedule (light on at 6 a.m.).

Organ cultures of calvarial bones. The technique for studying organ cultures of neonatal murine calvarial bones has been described previously with modification (34). The bones were removed from the calvaria of 3-day-old male wild-type and $AR^{-/Y}$ mice and then cultured in Biggers, Gwatkins, Judah media with the Fitton-Jackson modification with 0.1% bovine serum albumin for 72 h in the presence or absence of DHT. After treatment, the calvaria were fixed for 24 h in 10% phosphate-buffered formalin. The calvaria were then embedded in paraffin, and 4-μm sections were cut and then stained with hematoxylin and eosin (H&E), Goldner trichrome, or von Kossa stain. Bone formation and mineralization were evaluated by histomorphometric assessment using a Nikon E400 microscope attached to an SPOT-RT slider charge-coupled device color video camera. Images of the sectioned calvaria were captured at ×20 objective magnification. Each captured image was then stored for future reference, and the area of new bone formation, expressed as new bone area (square millimeters, 10^3), and the number of bone-lining cells, expressed as cells per 0.3-mm bone, were measured by using image analysis software, Image-Pro Plus (Media Cybernetics, Silver Spring, MD).

Bone microcomputed tomography and histomorphometry. Calvarial bones from the 8-, 12-, and 50-week-old male wild-type and $AR^{-/Y}$ mice were scanned on a Skyscan 1076 instrument (Skyscan). Image acquisition of the head was performed using ×25 magnification at 45 kV and 222 μA, with a 0.45° rotation between frames to obtain two-dimensional images. Three-dimensional reconstruction and quantitative analyses were performed on a computer (Dell) using the NRecon, ANT, and CTAn software supplied with the Skyscan instrument. Quantitative histomorphometric measurements were made in a blinded manner

using the computerized image analysis system. In the parietal bone of the calvaria, measurements were confined to the region located halfway between the sagittal and temporal sutures along a length of 2,100 mm on both sides of the sagittal suture. Width measurements were made every 10 mm in the region of interest. The terminology and units used are those recommended by the Histomorphometry Nomenclature Committee of the American Society for Bone and Mineral Research (41).

Immunohistochemistry. Specimens were fixed in 4% paraformaldehyde, permeabilized with 0.2% Triton X-100, embedded in paraffin, and sectioned (5 μm). Upon antigen retrieval with 20 mM sodium citrate (pH 6) and incubation with an AR antibody (N-20; Santa Cruz), sections were stained using biotin-coupled secondary antibodies (Jackson Immunoresearch Laboratories), together with a Vectastain ABC kit (Vector Laboratories, Burlingame, CA). Pictures were taken and acquired by using ×20 objective lenses with a Nikon E400 microscope attached to an SPOT-RT slider charge-coupled device color video camera and Image-Pro Plus software at room temperature.

Cell culture, transfection, plasmids, and siRNA. MC3T3-E1 cells were kindly provided by Renny T. Franceschi, University of Michigan, Ann Arbor. MC3T3-E1 cells were maintained in α-minimal essential growth medium (Invitrogen) with 10% fetal bovine serum (FBS; Clonetics). For primary osteoblast cell culture, the calvaria were then subjected to a series of collagenase digestions. Cells released from calvaria digested with 0.1% collagenase A and 0.2% dispase were neutralized with FBS, filtered through sterile polypropylene mesh, and resuspended in medium containing 10% FBS. Osteoblastic cells from the second to fifth fractions were pooled and counted following trypan blue staining to exclude nonviable cells and then diluted to 2×10^4 cells per ml on six-well plates for the osteoblastic differentiation assay. Where indicated, calf intestinal TNSALP (New England Biolabs) was added to the medium at 0.5 to 1.0 U/ml. The transfection protocol and reporter gene assays were performed as previously described (24). The inducing agents were replaced with each medium change (3 to 4 days). Stable clones were obtained after selection with puromycin. Control clones were obtained after transfecting empty or scramble vectors. For transient transfection of AR siRNA, the SMARTpool AR was used (Upstate Biotechnology). The pSuperior.retro.puro vector (OligoEngine) was used for the expression of siRNA in primary osteoblast cells. The AR siRNA vector was generated by a gene-specific insert (5′-GGGCCCTATCCCAGTCCCACTTGCTCGAGCAAG TGGGACTGGGATAGGGCTTTTTGAATTC-3′) to target AR. A scrambled control vector was constructed using an insert (5′-GTGTCTGTAGGAGTCAT CC-3′) with no significant homology to any mammalian gene sequence.

Mineralization assay. On day 2 postplating, the medium was replaced with osteogenic medium with 10% charcoal-coated-dextran-treated FBS, 50 μg of ascorbic acid-2-phosphate (Sigma)/ml, and 10 mM β-glycerol phosphate (Sigma). The following day, when cells were >90% confluent, hormones or vehicle (ethanol) were added. Von Kossa staining was performed by incubating the cells in 2.5% silver nitrate for 1 h in the dark. The samples were then exposed to light to produce black precipitation. Calcium deposition was assessed by using a liquid calcium detection kit (Human Biotech, Germany). Alizarin red staining was performed by incubating the cells with 2.5% alizarin red (Sigma).

Analysis of ALP. ALP staining was performed by using a Fast Violet/naphthol kit (85L-3R; Sigma). The ALP activity was assayed in cell lysates by determining the release of *p*-nitrophenol from *p*-nitrophenyl phosphate at 37°C and pH 10.5. ALP activity was measured in duplicate and reported as nanomoles per minute of incubation time per milligram of protein.

Immunoblotting. Western blot analysis was performed as previously described (24). For phosphate treatment of MC3T3-E1 cells, confluent cells were treated with 10 mM sodium phosphate for 3 days. Cell lysates were then collected to assess AR protein levels. In brief, cell pellets were lysed, and the protein content was assessed with protein assay reagent (Pierce, Rockford, IL). After separation by sodium dodecyl sulfate-polyacrylamide gel electrophoresis, proteins were transferred to Hybond-P membranes (Amersham-Pharmacia Biotech, Piscataway, NJ) and assayed with an antiserum against AR (N-20; Santa Cruz) using a horseradish peroxidase-conjugated, anti-rabbit secondary antiserum (Amersham), detected using an ECL Plus kit (Amersham) and quantified by using Bio-Rad Quantity One software. Membranes were reprobed for β-tubulin (I-19; Santa Cruz) for normalization. The results were expressed as the fold increase over cells harvested on day 1.

RNA isolation and real-time RT-PCR analysis. Total RNA was isolated using TRIzol reagent (Life Technologies, Frederick, MD) and reverse transcribed. Real-time reverse transcription-PCR (RT-PCR) was performed by using a Sybr green PCR master mix kit (PE Applied Biosystems, Foster City, CA) as previously described (25). Sequence analysis was performed by using an ABI Prism 7700 sequence detection system (PE Applied Biosystems). The sequences of all
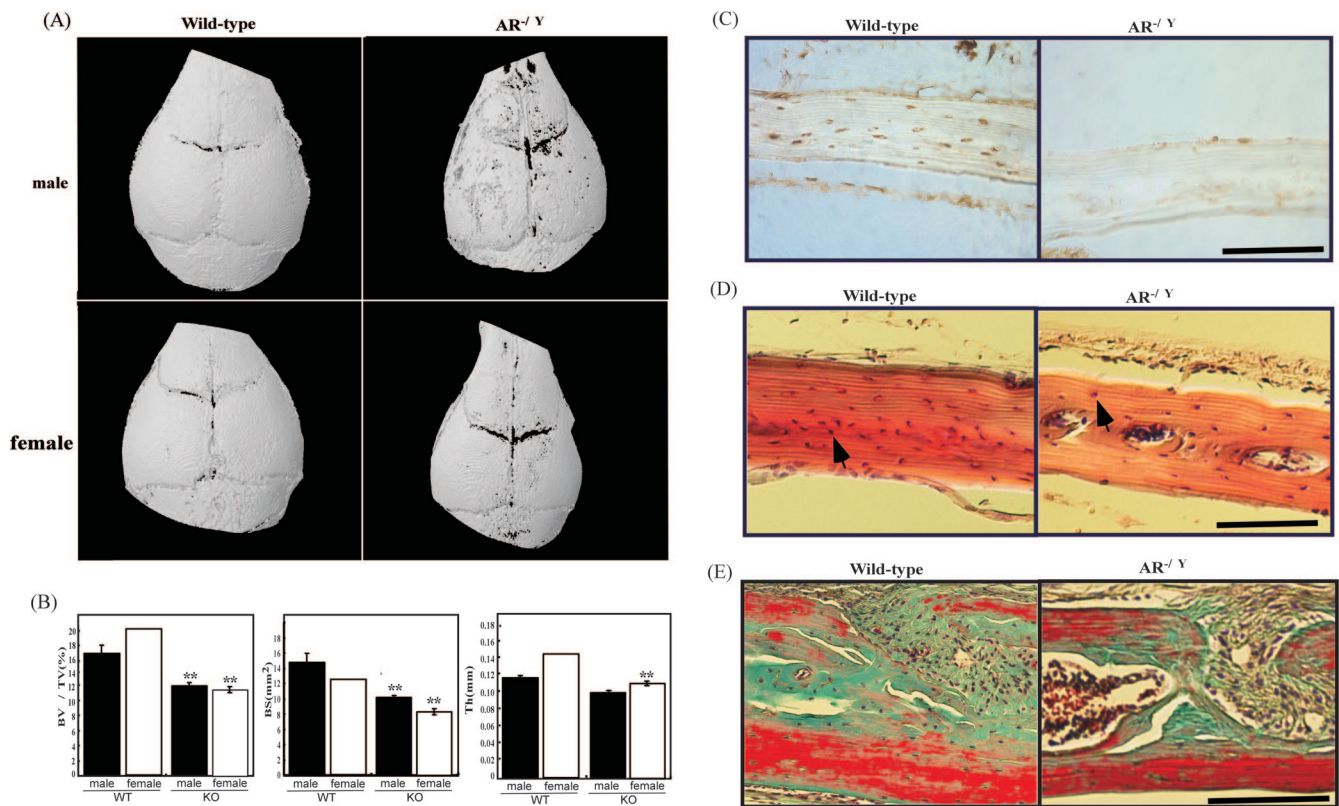
(A)

(B)

(C)

(D)

(E)

FIG. 1. Altered calvarial morphology and reduced mineralization observed in AR$^{-/Y}$ mice. (A) Three-dimensional computer tomography images of the calvaria from representative 8-week-old male and female wild-type and ARKO mice. (B) Quantitative micro CT analysis measurements of calvarial bone volume, thickness, and bone surface values are provided for each skull from 8-week-old male and female wild-type and ARKO mice. ($n = 6$ to 8 animals per genotype; Student t test, $P < 0.01$). Error bars represent ± the standard deviation (SD). ∗∗, Samples significantly different from wild-type mice. (C) Immunochemical identification of AR (brown color) in calvarial bones. The calvaria of 8-week-old male wild-type and AR$^{-/Y}$ mice were used for the immunodetection of AR in bone cells. (D) H&E staining of calvarial sections from 8-week-old male wild-type and AR$^{-/Y}$ mice. Unlike wild-type mice, fewer osteocytes (arrow) are evident on the bone matrix in AR$^{-/Y}$ mice. (E) Goldner's trichrome staining of calvarial sections from 12-week-old male wild-type and AR$^{-/Y}$ mice. Bar, 50 μm. Larger areas of mineralized bone (green) and osteoid/collagen (red) are clearly visible above the bone surface in the wild-type mouse section compared to the AR$^{-/Y}$ mouse section. The irregular shape of the intersutural mesenchyme with large nuclei (dark purple) and decreased number of osteoblasts and osteocytes in the calvaria of male in AR$^{-/Y}$ mice indicate decreased bone mineralization.

primers used in the present study are listed in Table S4 in the supplemental material.

Luciferase assay. MC3T3-E1 cells cotransfected with serial deletion *AKP2* promoter luciferase reporter plasmids and AR expressing plasmid were treated with or without DHT for 48 h and measured for firefly luciferase activity by using a dual luciferase assay kit (Promega) with *Renilla* luciferase used as an internal control to confirm transfection efficiency as previously described (26).

ChIP assay. Chromatin immunoprecipitation (ChIP) assays were performed as described previously (29) with modifications. Cell lysates were precleared sequentially with normal rabbit immunoglobulin G (IgG; sc-2027; Santa Cruz) and protein A-agarose using an EZ ChIP kit (Upstate catalog no. 17-371). The cell lysates were then incubated overnight at 4°C with 2.0 μg of anti-AR antibody (N-20; Santa Cruz). IgG antibody was added for the negative control cell lysate. The primer pairs, which span the region from position −1412 to position −1181 of the AKP2 promoter, were used for PCR amplification.

Phosphate analysis. Cells were seeded at 10^4 cells per well on a 12-well culture plate. Growth media were changed to mineralizing medium that was replaced every 3 days for 6 days. Cytosolic fractions were extracted by using a subcellular proteome extraction kit (Calbiochem). P_i was measured by using a PiBlue phosphate assay kit (BioAssay Systems), and the optical density at 620 nm was determined by using an enzyme-linked immunosorbent assay reader (Wallac; Victor^2 V). The data were expressed as nanomoles of phosphate/microgram of protein in each well. For phosphate inhibition analysis, cells were treated with 3 mM phosphonoformic acid (PFA; Sigma) 3 h before phosphate treatment.

Immunocytofluorescence. MC3T3-E1 cells were seeded in α-minimal essential medium with 10% FBS onto four-well LabTek chamber slides (Nalge) and treated with 10 nM DHT or 1 mM P_i overnight. Cells were then fixed, and immunostaining was performed by incubating cells with anti-AR antibody (N-20; Santa Cruz), followed by incubation with fluorescein-conjugated goat anti-rabbit antibody. Slides were mounted with mounting medium containing DAPI (4′,6′-diamidino-2-phenylindole; Vector Laboratories) and sealed, and the images were acquired with a C1 laser scanning confocal microscope (Nikon, Melville, NY).

Statistical analyses. All values are the means ± the standard deviations (SD) of replicate samples ($n = 3$ to 6, depending on the experiment), and experiments were repeated a minimum of three times. Differences between two groups were assessed by using the unpaired two-tailed Student t test or among more than two groups by analysis of variance. In all statistical comparisons, $P < 0.05$ was defined as a significant difference. SigmaStat statistics software (version 2.0; SPSS) was used for all calculations.

RESULTS

Androgen/AR contributes to new bone formation and mineralization in calvarial bones. To investigate whether the abnormal phenotype occurred in the calvaria of ARKO mice, skull
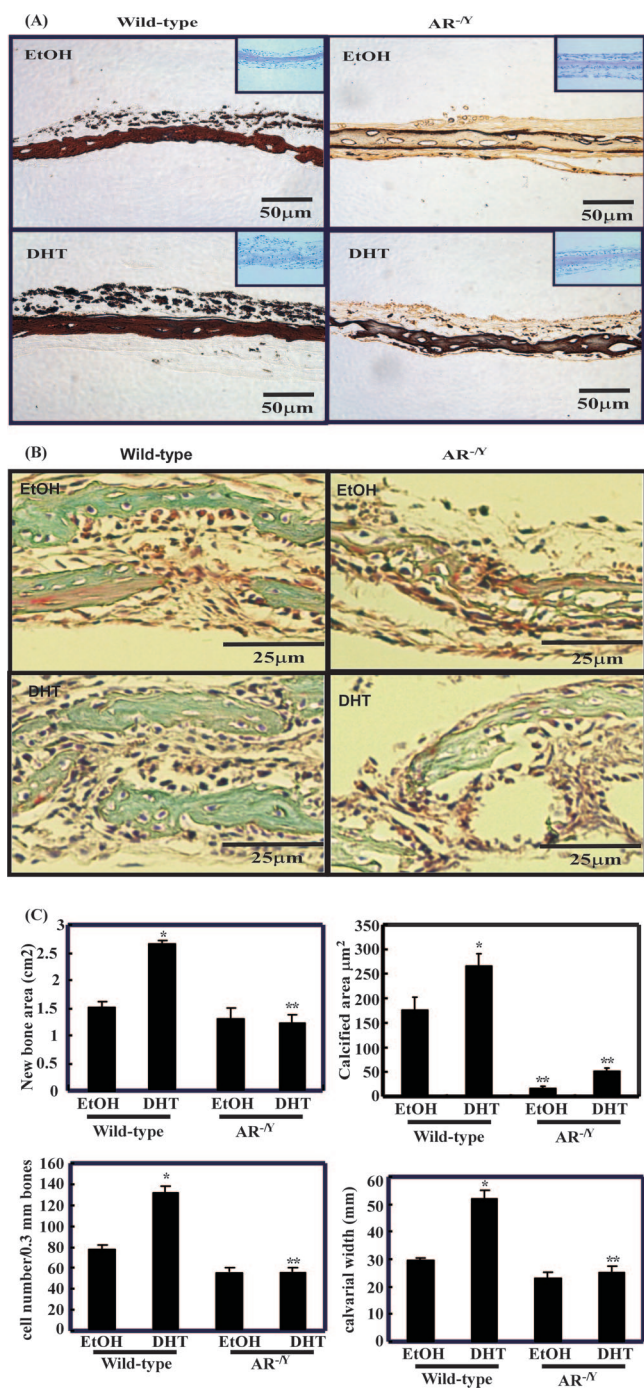
FIG. 2. Androgen/AR promotes new bone formation; mineralization, suture width, and osteocyte number were also evaluated. Areas of mineralized bone were stained with Von Kossa (silver nitrate with black color) (A) and Goldner's trichrome (green color) (B) in calvaria from neonatal male wild-type and $AR^{-/Y}$ mice cultured without (top) or with (bottom) DHT. The inset in panel A shows an expanded view of the calvarial bones with H&E staining. Bar, 50 μm. (C) Histomorphometric measurements of new bone area (calculated by subtracting the original bone area from the total bone area) and calcified area (μm² per 400 μm² calculated by using Image Pro Plus software) of calvarial bones from $AR^{-/Y}$ mice showed no response to DHT and significantly less mineral deposition and relatively less new bone area than wild-type mice. Similarly, smaller suture width (the distance between the two outer edges of the coronal suture) and numbers of cells (calculated by dividing the cell number by the section length per 0.3

bones from 8- to 10-week-old male and female ARKO mice and wild-type littermates were assessed by microcomputed tomography scan analysis. The findings revealed delayed mineralization of the skull vault, reduced bone volume and surface area, and thickness in the calvaria of both male and female ARKO mice compared to wild-type littermates (Fig. 1A and B). Histomorphometric analysis indicated that calvaria from 8-week-old male and female ARKO mice were significantly narrower in width and had a smaller bone area, osteoid surface, lower osteocyte number, and higher osteoclasts per bone area than wild-type mice (see Table S1 in the supplemental material). We used highly sensitive immunohistochemistry to investigate the expression profile of AR in mature calvarial bone in 8-week-old mice to determine whether $AR^{-/Y}$ mice osteoblasts are functional. AR protein expression appears to be abundant in the osteoblasts and osteocytes of calvarial sections from wild-type mice (Fig. 1C). In comparison, AR expression is undetectable in calvarial sections from $AR^{-/Y}$ mice (Fig. 1C). In addition, $AR^{-/Y}$ mice exhibited clear evidence of decreased numbers of osteoblasts and osteocytes in the calvaria (Fig. 1D). The irregular shape of the intersutural mesenchyme with large nuclei and reduction of mineralized bone and osteoid were observed in the calvaria of $AR^{-/Y}$ mice (Fig. 1E). Progressive abnormalities in the calvaria were also observed in 30- and 50-week-old $AR^{-/Y}$ mice (see Fig. S1 in the supplemental material), suggesting that loss of AR has a negative effect on bone quality parameters in developing skeletal tissue.

We then assessed the effect of androgen/AR on bone formation in cultures of neonatal calvarial bones from wild-type and $AR^{-/Y}$ mice for 5 days by using in vitro organ culture as previously described (34, 50). Decreased bone mineralization was observed in the skull of $AR^{-/Y}$ mice as assessed by Von Kossa (Fig. 2A) and Goldner's trichrome (Fig. 2B) staining. Quantitative histomorphometric analysis revealed that new bone areas increased with DHT treatment in wild-type calvaria, and loss of AR impaired DHT-stimulated bone formation (Fig. 2C), suggesting that AR plays an important role in androgen-mediated bone formation. The calcified area was significantly reduced in $AR^{-/Y}$ calvarial bones, and osteocytes in the control and DHT-treated wild-type calvaria were clearly cuboidal, in contrast to the flat morphology observed in $AR^{-/Y}$ calvaria (Fig. 2B). In addition, we found that DHT, but not control media, caused a significant increase in the number of bone-lining cells and suture width in wild-type compared to $AR^{-/Y}$ mice calvarial organ cultures (Fig. 2C). These results suggest that the loss of AR not only causes inhibition of androgen action to promote new bone formation but also results in a significant decrease in osteoblast activity required for differentiation and mineralization.

The extent of androgen-mediated mineralization in osteoblasts depends on timing of androgen administration and AR expression. The effect of androgen exposure on osteoblasts and the androgen responsiveness of the bone cells were char-

mm) were detected in calvarial bones from $AR^{-/Y}$ mice compared to wild-type mice. Error bars represent ± the SD. *, Samples significantly different from ethanol treatment ($P < 0.05$); **, samples significantly different from wild-type mice ($P < 0.05$).
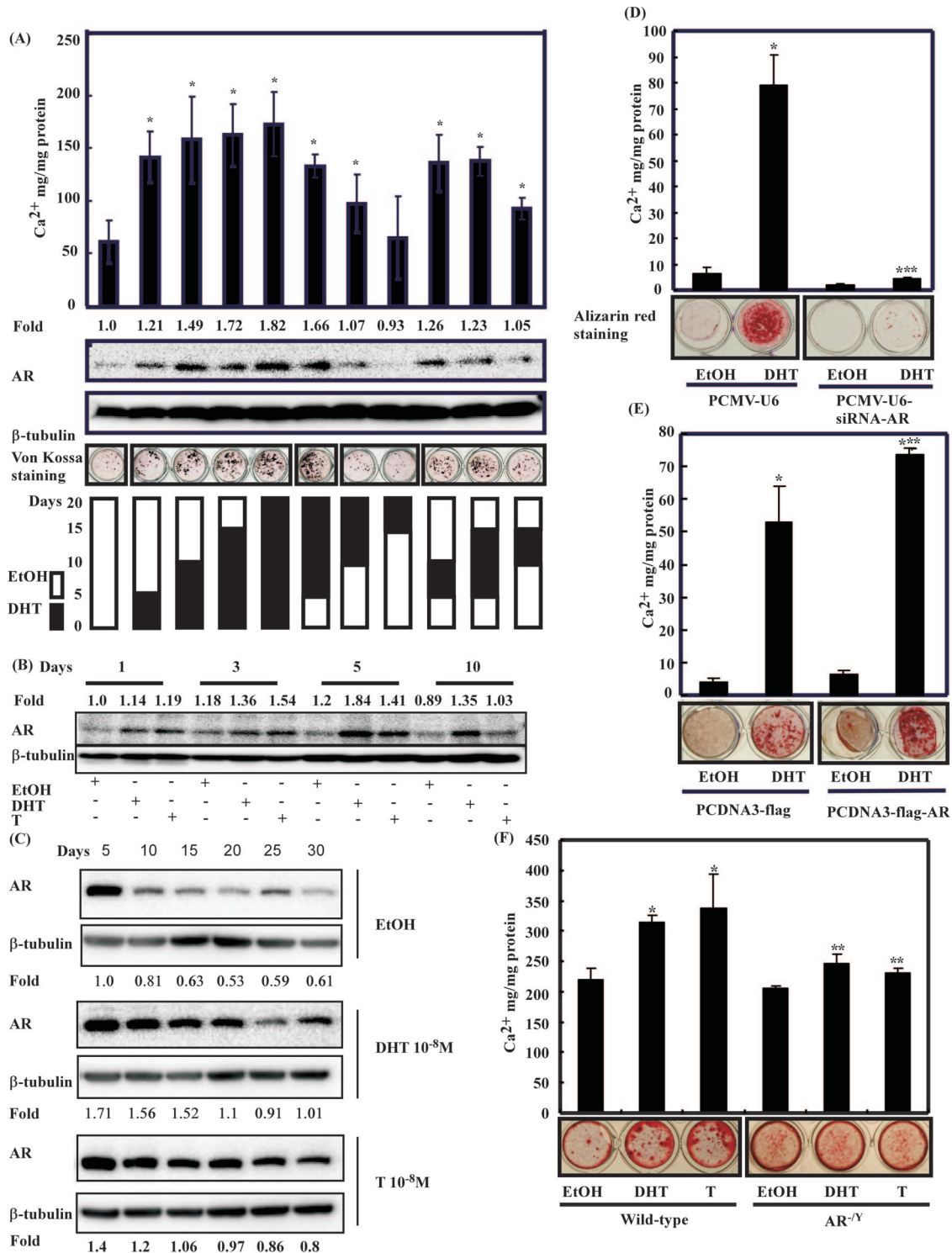
FIG. 3. The extent of mineralization in response to androgens depends on the timing of androgen administration and the expression profile of AR expression during osteoblast differentiation. (A) The top panel represents a calcium deposition assay for calcium levels, the upper middle panels represent Western blot for AR and β-tubulin protein, and the lower middle panel represents von Kossa staining for osteoblast mineralization. On the bottom panel, open bars represent cells grown in ethanol-containing medium, and solid bars represent cells grown in androgen-containing medium to which 10^{-8} M DHT was added on day 0 (0 to 5, 0 to 10, 0 to 15, and 0 to 20), day 5 (5 to 10, 5 to 15, and 5 to 20), day 10 (10 to 15 and 10 to 20), and day 15 (15 to 20). (B and C) Analysis of AR protein levels in MC3T3-E1 cell culture with ethanol, DHT, or testosterone (T) in osteogenic medium. β-Tubulin was used as a loading control. AR levels were readily detected in the first 5 days then decreased during maturation and mineralization. Error bars represent ± the SD. Asterisks (∗) mark samples significantly different from ethanol treatment ($P <$ 0.05). Cell lysates were collected at days 1, 3, 5, and 10 (B) or at 5-day intervals from day 0 to day 30 (C) to detect AR expression by Western blot analysis. The optical densities obtained for AR bands from ethanol-treated cultures were normalized by β-tubulin expression and set as 1. (D to

acterized using MC3T3-E1 cells as a model of osteoblast differentiation. MC3T3-E1 cells are androgen responsive and express high levels of ALP and AR (16, 36). Calcium deposition was significantly greater when cells were exposed to DHT from day 1 postplating for a treatment period of 20 days [(3.3 ± 0.35)-fold] than in vehicle-treated cells (Fig. 3A, bottom panel). Exposure of cells to DHT during days 5 to 10, 5 to 15, or 5 to 20 postplating resulted in a two- to threefold increase in mineralization compared to vehicle-treated cells. In comparison, exposure of cells to DHT during days 10 to 15 or days 15 to 20 resulted in a level of calcium deposition equivalent to vehicle-treated cells. In addition, these results show that androgen treatment during days 0 to 5 is enough for calcium deposition. The extent of androgen-mediated mineralization correlates with the level of AR expression. As shown in Fig. 3B and C, the relationship between androgen responsiveness and AR levels was further characterized by determining the AR protein level in MC3T3-E1 cells at different assay time points. The expression of AR in MC3T3-E1 cells increased between days 1 and 5 postplating reached a maximum level after day 5 and diminished gradually from day 10 to day 30. Exposure of cells to testosterone or DHT resulted in a significant increase in the level of AR by day 1 compared to vehicle-treated cells during osteoblast differentiation (Fig. 3C). To determine whether AR is required for osteoblast mineralization, we used specific RNA interference against AR (siRNA-AR) to block AR expression in MC3T3-E1 cells. We showed that inhibition of AR expression decreased androgen-mediated cell mineralization in MC3T3-E1 cells (Fig. 3D). By comparison, the enhanced expression of constitutively active AR increased the basal levels of calcium deposition in MC3T3-E1 cells stably transfected with AR and DHT further enhanced calcium deposition (Fig. 3E). To further study the role of AR in androgen-mediated osteoblast mineralization, calvarial osteoblasts isolated from wild-type mice and AR$^{-/Y}$ mice were treated with DHT or testosterone, and cell mineralization was measured by alizarin red staining. As shown in Fig. 3F, androgen-mediated calcium deposition was significantly greater in calvarial osteoblasts isolated from wild-type mice compared to those from AR$^{-/Y}$ mice.

Identification of androgen/AR-regulated genes in osteoblasts. Microarray analysis was used to identify genes involved in the progression of androgen-mediated osteoblast differentiation, particularly those with a role in bone mineralization. Primary neonatal calvarial osteoblast cells from wild-type and AR$^{-/Y}$ mice were isolated and then exposed to osteogenic medium to induce mineralization in the presence or absence of DHT. Microarrays were then used to identify specific genes differentially expressed between wild-type and AR$^{-/Y}$ osteoblasts (see Table S2 in the supplemental material). MC3T3-E1-AR cells overexpressing AR were used in a parallel screen to identify genes highly expressed. Real-time PCR was used to confirm the presence of all probe sets in the samples. We found that the expression of the *AKP2* gene and the small integrin-binding ligand, N-linked glycoprotein (SIBLING) gene family, which includes secreted phosphoprotein 1 (*OPN/SPP1*), bone sialoprotein (*BSP*), dentin matrix protein 1 (*DMP1*), and dentin sialophosphoprotein (*DSPP*), decreased significantly in calvarial cells from AR$^{-/Y}$ mice compared to those from wild-type mice (Fig. 4A, left panel and see Fig. S2A in the supplemental material). The expression profiles of these genes during androgen-mediated osteoblast differentiation was investigated, and gene expressions were analyzed in MC3T3-E1 cells on days 1 to 30 in the presence or absence of DHT by using real-time RT PCR. We found that the expression patterns of all of these genes regulated by DHT have the highest peak expression around days 15 except for *DMP1* (around days 30), which correlates with the differentiation of osteoblasts and the onset of mineralization (see Fig. S2C in the supplemental material). To determine whether AR is involved in the regulation of expression of these genes, MC3T3-E1 cells were transfected with siRNA-AR to block AR expression. While inhibition of AR expression by siRNA-AR decreased the expression of *AKP2* gene and the SIBLING genes, exposure of MC3T3-E1 cells with control-siRNA to DHT induced the expression of these genes from 2- to 10-fold (Fig. 4B, left panel, and see Fig. S2B in the supplemental material). In addition, we were able to observe the dose-dependent effects of androgen/AR on the induction of *AKP2* gene expression (Fig. 4B, right panel). To better understand the regulation of the *AKP2* gene and the SIBLING genes, approximately 3 kb of sequence upstream of the putative transcriptional start sites of these genes was examined for homology to the androgen response element (ARE) consensus motif from the TRANSFAC database (37). All of these genes contain one or more motifs comprising at least 75% corresponding to the consensus ARE sequence (see Fig. S2D in the supplemental material). In addition, the expression of transiently transfected *AKP2* gene promoter-reporter (luciferase) constructs (39) in the osteoblasts was also androgen dependent, and when the cells were transfected with the vector containing *AKP2* gene promoter-upstream fragment extending from positions −4556 and −1776, which includes putative ARE consensus sites at −2284, DHT elicited an ∼3-fold induction of luciferase activity (Fig. 4C). To test whether AR was recruited to the putative ARE consensus sites of these gene promoters in osteoblasts in an androgen-dependent manner, ChIP analysis was performed. AR was found, by PCR detection after anti-AR antibody ChIP, to be associated in situ with the *AKP2* gene promoter in the presence of DHT (Fig. 4D). Similar results were obtained in SIBLING gene promoters (see Fig. S2E in the supplemental material). To examine whether the *AKP2* gene expressed in other tissues is also regulated by AR, the calvaria, tibias, femurs, cartilage, and livers from wild-type and AR$^{-/Y}$ mice

---

F) Mineralization analysis of MC3T3-E1 cells stably transfected with siRNA-control (pCMV-U6) or siRNA-AR (D), control vector (pCDNA-flag) or AR-expressing plasmid (pCDNA-flag-AR) (E), and primary osteoblasts from wild-type and AR$^{-/Y}$ mice stimulated with or without 10^{-8} M of DHT or T (F) in differentiation medium for 30 days. Cells were fixed and stained with alizarin red S for mineralized matrix, and the calcium amounts were determined by the colorimetric method. ∗∗∗, Samples significantly different from parent vector control ($P < 0.05$); ∗∗, samples significantly different from wild-type mice ($P < 0.05$).
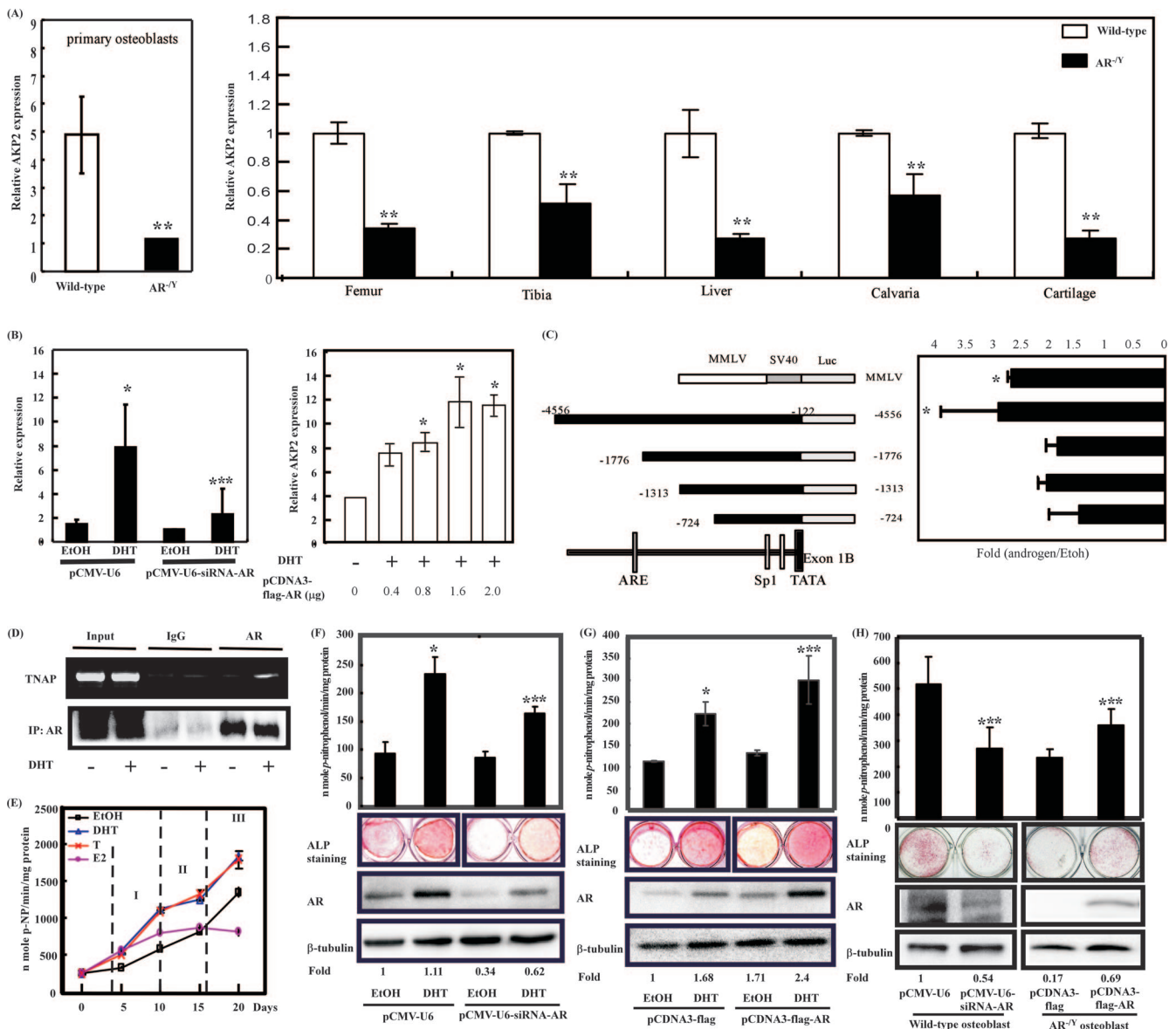
FIG. 4. AR is required for androgen-mediated ALP activity during osteoblast differentiation. (A) The relative AKP2 gene expression in the calvaria, tibias, femurs, cartilage, livers, and primary osteoblasts from 5- to 6-week-old wild-type and $AR^{-/Y}$ mice was determined by real-time PCR. (B) MC3T3-E1 cells stably transfected with siRNA-control (pCMV-U6) or siRNA-AR cells were stimulated with or without 10^{-8} M DHT in differentiation medium (left panel). The induction of AKP2 gene by androgen/AR was assayed in MC3T3-E1 cells transfected with a dose-dependent amount of pCDNA3-AR expression vector (right panel). The relative mRNA expression of AKP2 gene was determined by real-time PCR. (C) Serial deletion analysis of the AKP2 gene promoter regulated by androgen/AR. Different AKP2 promoter constructs were cotransfected with AR expression vector into MC3T3-E1 cells cultured in the presence or absence of DHT, and the luciferase activities were measured. MMTV-luc was used as a positive control for AR transactivation activity. (D) ChIP analysis of AR occupation of the AKP2 promoter in osteoblasts cultured in the presence or absence of DHT. Immunoprecipitation (IP) was performed with anti-AR antibody. (E) MC3T3-E1 cells were induced to undergo osteogenic differentiation in the presence of 10^{-8} M of ethanol, DHT, T, and E2, resulting in proliferation (stage I), maturation (stage II), mineralization (stage III), and activation of TNSALP, as detected by an ALP activity assay. Analysis of TNSALP activity and AR expression in MC3T3-E1 cells stably transfected with siRNA-control (pCMV-U6) or siRNA-AR (F) and control vector (pCDNA-flag) or AR-expressing plasmid (pCDNA-flag-AR) (G) was carried out. (H) Analysis of TNSALP activity and AR expression in primary wild-type osteoblasts transfected with siRNA-control (pCMV-U6) or siRNA-AR and $AR^{-/Y}$ osteoblasts transfected with control vector or AR-expressing plasmid stimulated with or without 10^{-8} M DHT in differentiation medium. Treated cells were fixed and stained, and the ALP activity was determined by incubating cell lysates with ALP substrates for colorimetric analysis. Western blot analysis was performed to determine AR expression. The optical densities obtained for AR bands from ethanol-treated cultures were normalized by using β-tubulin expression levels and set as 1. The data are representative of at least three independent experiments, and error bars represent ± the SD. *, Samples significantly different from ethanol treatment ($P < 0.05$); **, samples significantly different from wild-type mice ($P < 0.05$); ***, samples significantly different from parent vector control ($P < 0.05$).

were used to analyze the mRNA expression level of AKP2. The results (Fig. 4A) showed that the expression level of *AKP2* gene was decreased in calvaria, tibias, femurs, cartilage, livers, and primary osteoblasts from $AR^{-/Y}$ mice compared to those from wild-type mice.

AR is required for androgen-mediated ALP activity during osteoblast mineralization. The action of androgens on TNSALP function during osteoblast differentiation and mineralization was investigated using MC3T3-E1 cells exposed to a variety of steroids and assessed for ALP activity every 5 days from day 0 to day 20. Figure 4E shows the promotion of ALP activity by testosterone and DHT in a temporal manner over successive developmental stages including proliferation (stage I, days 4 to 10), bone matrix formation and/or maturation (stage II, days 10 to 16), and mineralization stages (stage III, days 16 to 20) (6). By comparison, the vehicle control had little effect on ALP activity. Activation of ALP by testosterone and DHT occurred between days 5 and 10, with activation reaching a peak around day 20. It appears that testosterone and DHT have more significant effects on ALP activity during osteoblast differentiation in MC3T3-E1 cells than does 17β-estradiol (E2). To investigate the role of AR in androgen-mediated ALP activity in osteoblast mineralization, we introduced the siRNA-AR or flag-AR vectors into MC3T3-E1 cells and assayed for androgen-induced ALP activity. After exposure of cells to DHT for 10 days, androgen-mediated ALP activity and staining were observed in parental cells and those overexpressing AR but not in AR knockdown cells (Fig. 4F and G). In addition, ALP activity and staining, which was suppressed in wild-type calvarial osteoblasts expressing siRNA-AR, increased in $AR^{-/Y}$ calvarial osteoblasts overexpressing AR (Fig. 4H). These results were confirmed by the finding that ALP activity was significantly lower in the calvaria but not in the serum from $AR^{-/Y}$ mice compared to wild-type mice (see Table S3 in the supplemental material).

Reciprocal regulation of phosphate level and AR expression. The process of osteoblast differentiation and matrix mineralization requires a rise in the level of TNSALP activity to generate P_i ions from the hydrolysis of extracellular inorganic pyrophosphate (PP_i) for deposition into the extracellular matrix (ECM) (9). To gain insight into the mechanisms underlying the regulation of TNSALP activity by androgen/AR, we measured the P_i levels in wild-type calvarial osteoblasts expressing siRNA-AR and in $AR^{-/Y}$ calvarial osteoblasts overexpressing AR in the presence or absence of DHT. The intracellular P_i concentration was significantly higher in $AR^{-/Y}$ osteoblasts overexpressing AR in the presence of DHT than in control or untreated cells (Fig. 5A). Suppression of AR expression with AR-specific siRNA impaired the response of wild-type osteoblasts to DHT, resulting in a lower level of P_i compared to control cells (Fig. 5A). We then investigated the role of TNSALP and phosphate transporters on androgen-mediated P_i uptake in MC3T3-E1 osteoblasts. This was achieved using levamisole (L) to inhibit TNSALP activity and phosphate transport inhibitor foscarnet (PFA) to block type III Na^+/P_i cotransporter function. As shown in Fig. 5B, the level of P_i was significantly lower in MC3T3-E1 osteoblasts treated with DHT and either L or PFA than in cells treated with DHT alone. This suggests that the androgen-mediated influx of P_i

into osteoblasts is regulated by TNSALP and phosphate transporters.

The ability of cells to respond to phosphate by the temporal coordination of gene expression and regulation of protein function is recognized as a requirement for mineralization in bone (4). To investigate whether the P_i generated by TNSALP influences the expression and function of AR, we examined the expression of AR in MC3T3-E1 osteoblasts responding to P_i only or β-glycerophosphate (β-GP), a provider of P_i ions and the proposed substrate of TNSALP, in the presence or absence of DHT. As shown in Fig. 5C, both sources of phosphate enhanced the level of AR expression in the presence or absence of DHT. AR expression was further enhanced with the ectopic expression of calf TNSALP in the presence of β-GP but was suppressed by L treatment (Fig. 5D). Similarly, PFA inhibits P_i-enhanced AR expression (Fig. 5E). In addition, both L and PFA blocked DHT induced mineralization of the ECM surrounding MC3T3-E1 osteoblasts (Fig. 5F). Interestingly, reporter gene assays and immunofluorescence studies using the anti-AR antibody showed that AR had a diffuse cytosolic distribution in vehicle-control cells. After treatment with P_i, a portion of AR translocated from cytosol to the cell nucleus and showed transactivation activity similar to DHT treatment (Fig. 5G and H).

TNSALP and P_i are necessary for AR-mediated bone mineralization. To determine the biological significance of the role of TNSALP in AR-mediated bone mineralization, we cultured MC3T3-E1 osteoblasts with knocked-down AR or vector control with β-GP in the presence or absence of DHT. As expected, mineralization was induced in the ECM surrounding MC3T3-E1 osteoblasts and was not induced in the ECM surrounding osteoblasts with knocked down AR (Fig. 6A and B). We also cultured control and AR knockdown osteoblasts with ectopic expression of calf intestine TNSALP plus β-GP or in the presence of P_i only. In both culture conditions, osteoblasts with knocked down AR showed mineralization in the surrounding ECM, albeit to a lesser extent than control osteoblasts (Fig. 6A and B). Taken together, these results show that the AR regulation of expression of bone-related proteins, such as TNSALP, is a necessary requirement for androgen-mediated osteoblast mineralization. It is possible that AR alters the capacity of TNSALP to cleave PP_i and hence alters the PP_i to P_i ratio in the bone microenvironment. We then investigated the effect of the TNSALP or P_i on mineralization from calvarial bone lacking AR. When calvarial bones of $AR^{-/Y}$ mice were cultured with ectopic expression of calf TNSALP or P_i in culture media, a partial rescue of bone loss in calvarial bones from $AR^{-/Y}$ mice was observed, as determined by the calcified area that remained mineralized as shown by Von Kossa and Goldner's trichrome staining (Fig. 6C).

DISCUSSION

The present study shows that the TNSALP level in calvarial osteoblasts (Fig. 4B) and calvaria (see Table S1 in the supplemental material) is significantly lower in $AR^{-/Y}$ mice, strongly suggesting that the trigger for androgen-mediated bone mineralization involves TNSALP. Although Akp2$^{Hpp/+}$ mice have ca. 50% of normal plasma ALP but display no other biochemical or skeletal abnormalities, recent studies showed that
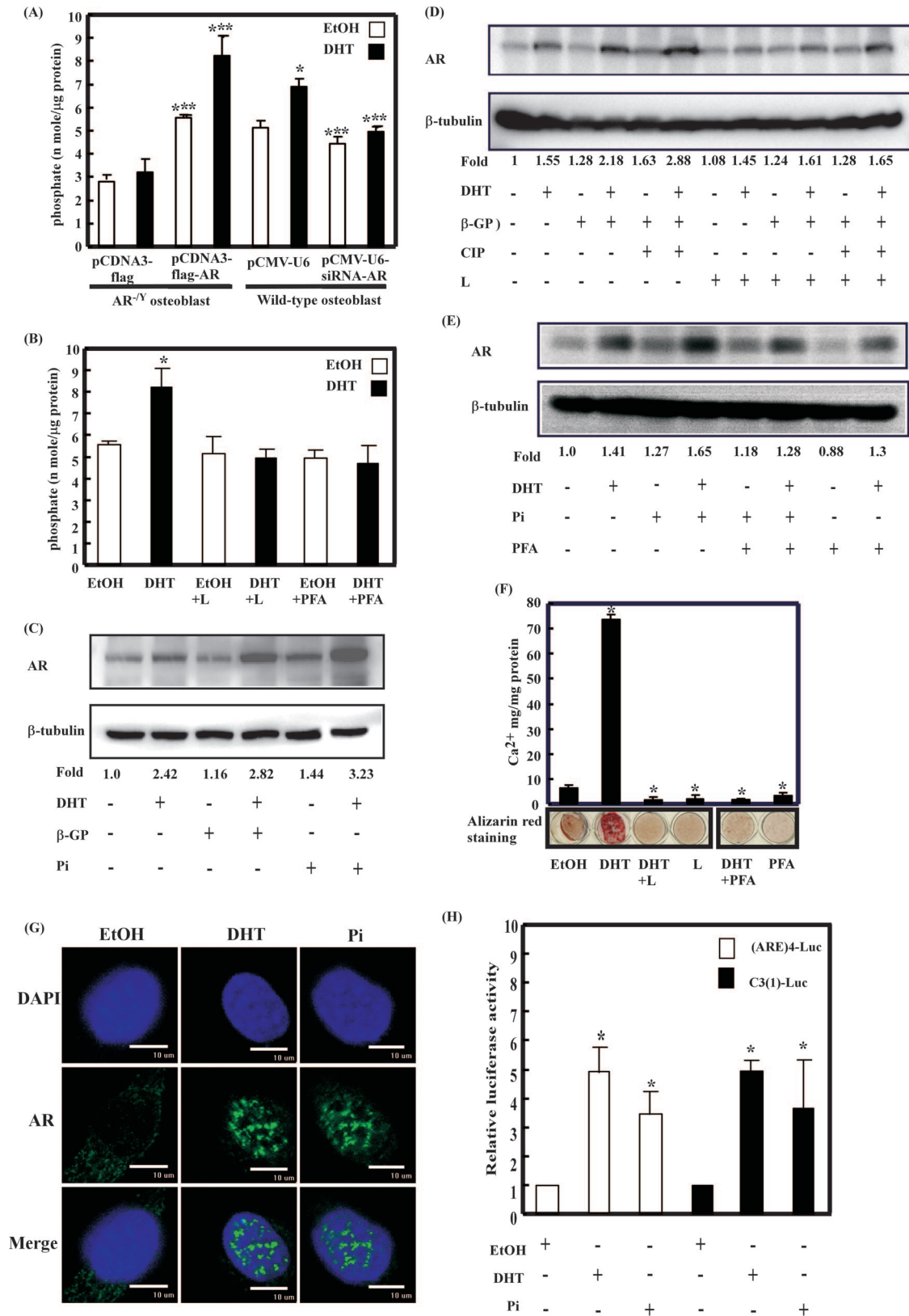
FIG. 5. Reciprocal regulation of AR and P_i. (A and B) Intracellular P_i concentration in primary wild-type osteoblasts transfected with siRNA-control (pCMV-U6) or siRNA-AR and in $AR^{-/Y}$ osteoblasts transfected with control vector or AR-expressing plasmid, stimulated with or without 10^{-8} M DHT (A) and in MC3T3-E1 cells treated with ethanol or DHT in combination with levamisole (L, ALP inhibitor) or PFA (a competitive inhibitor of type III Na^+/P_i cotransporters) (B) was measured after 9 days of treatment. Note the significant increase in intracellular P_i concentration in DHT-treated cells, whereas L and PFA decreased the P_i concentration. The data are representative of at least three

Akp2$^{Hpp/Hpp}$ mice, with ca. 10% of normal ALP activity, develop late-onset skeletal disease, notably defective endochondral ossification, and bone mineralization that leads to arthropathies of the knees and shoulders (19). The biological significance of the TNSALP regulated by AR to promote bone mineralization in vivo was further supported by castration of male Akp2$^{Hpp/Hpp}$ mice, which have accelerated defective bone mineralization (unpublished data). The main function of TNSALP is to catalyze the hydrolysis of pyrophosphate, generated by nucleotide pyrophophatase phosphodiesterase 1 (NPP1)/PC-1 and transported by ANK (22). The action of TNSALP increases the intracellular level of P_i and thereby raises the ratio of P_i to PP_i. It is unknown whether the ratio of P_i to PP_i is altered in the bone microenvironment of AR$^{-/y}$ mice and whether NPP1 and ANK are involved in AR-mediated bone mineralization; further investigation is required to elucidate these processes. Although the loss of AR has a detrimental effect on bone mineralization, the high TNSALP and/or P_i content rescue of the hypomineralization in AR$^{-/y}$ mice suggests that the level of P_i, possibly generated by TNSALP, is critical for AR-mediated bone mineralization in the ECM. This finding is in agreement with previous studies showing that the phosphate is required to trigger bone mineralization (35). We also showed that androgen induces an increase in the level of P_i, which may in turn promote AR nuclear translocation and activity. The contribution of P_i-mediated androgen/AR-regulated molecular events associated with the bone mineralization process remains to be further investigated.

Our results show that androgen administration enhances the capacity of AR to promote mineralization in a time- and/or stage-dependent manner. This finding is consistent with previous results showing that androgens promote mineralization by osteoblastic cells (48). Although it is possible that the mineralization effects seen in the culture system in vitro may be partly due to the effects of androgen/AR on the cell proliferation, survival, and differentiation, calvarial organ culture assays from ARKO mice clearly demonstrated that androgen/AR is required for promoting bone mineralization. We further indicate that the level of AR increases dramatically after exposure of MC3T3-E1 cells to androgen (DHT or testosterone) and that a dramatic androgen-independent increase in AR occurs during early maturation that gradually decreases during late maturation and mineralization (Fig. 3B and C). Despite the early androgen-dependent or -independent increase in AR protein, previous studies show that MC3T3-E1 cells fail to manifest a classic androgen response within the first 3 days after plating, whereas cells treated with dexamethasone did exhibit a response (2). This delayed response to androgen agrees with previous studies on human osteoblastic cells, which showed that increasing the level of AR by cotransfection with an AR expression plasmid enabled these cells to become androgen responsive (30, 58). Together, these findings suggest that an increase in the level of AR is essential for promoting androgen-mediated gene expression at a specific stage in osteoblastic cells.

Indeed, we also demonstrated that androgen treatments from days 0 to 5 were sufficient to promote mineralization of osteoblasts in vitro, a previously unrecognized aspect of androgen action. Therefore, the timing of early exposure of osteoblasts to androgen is critical to achieve the threshold level of AR required to activate differentiation markers, such as TNSALP, which is highly expressed in the maturation and mineralization stages. Thus, the net effect of androgens on mineralization depends on the timing of androgen exposure for stimulation of appropriate levels of AR and suggests that various amounts of AR may constrain mineralization at the earliest stage but induce at the later stages, an idea further supported by the results that the expression of androgen-mediated target genes are highly active in the later stage of osteoblast maturation (Fig. 4E and see Fig. S1C in the supplemental material). In addition, we were able to observe in MC3T3-E1 osteoblast cells significantly increasing AR expression level that reached a maximum level between days 5 and 10 upon stimulation by DHT but not in control or E2-treated groups. According to Ikegami's results, the mRNA level of ER was not altered by 10^{-8} M E2 treatment in MC3T3-E1 osteoblast cells, and ER protein expression was detectable in a heterogeneous pattern but not detectable in all cells (21). Furthermore, the ability of E2 to enhance ALP activity stimulated by 1,25-dihydroxyvitamin D$_3$ was dependent on the presence of dexamethasone treatment, a finding which has also been reported in human osteoblasts (43). Together, these results may provide evidence of possible mechanisms by which the ALP activity increased by DHT between days 5 and 10 can be observed but not by E2-treated or control groups in MC3T3-E1 cells. Taken together, the hormonal responsiveness of osteoblastic cells depends on receptor number and the stage of maturation of the cells when they are exposed to hormone.

---

independent experiments and error bars represent ± the SD. ∗, Samples significantly different from ethanol treatment ($P < 0.05$); ∗∗∗, samples significantly different from parent vector control ($P < 0.05$). (C to E) Analysis of AR protein levels in MC3T3-E1 cells treated with ethanol or DHT for 3 days in combination with β-glycerophosphate (β-GP) or phosphate (P_i) (C); β-GP, β-GP+calf intestine TNSALP (CIP), L, β-GP+L, or β-GP+CIP+L (D); or P_i, P_i+PFA, or PFA (E). For PFA and L treatment, cells were preincubated for 3 h. Cell lysates were collected at day 3, and Western blot analysis was performed to determine AR expression. The optical densities obtained for AR bands from ethanol-treated cultures were normalized using β-tubulin expression and set as 1. (F) MC3T3-E1 cells were treated with ethanol, DHT, DHT+L, L, DHT+PFA, or PFA for 30 days. Cells were then fixed, and calcium levels were determined by staining with alizarin red S for colorimetric analyses. The data are representative of at least three independent experiments and error bars represent ± the SD. ∗, Samples significantly different from ethanol treatment ($P < 0.05$). (G) Immunofluorescence analysis of AR nuclear translocation in osteoblasts regulated by P_i. MC3T3-E1 cells in separate culture dishes were treated with ethanol, DHT, or P_i and treated with the anti-AR antibody as indicated in the upper panel. The upper panel shows cells stained with DAPI. (H) MC3T3-E1 cells transfected with different ARE luciferase reporters were treated with ethanol, DHT, or P_i and lysed for luciferase activity. The reporter LUC activity from AR reporter gene was normalized by control LUC activity. After the LUC activity was measured, values relative to ethanol were calculated. The data are representative of at least three independent experiments and error bars represent ± the SD. ∗, Samples significantly different from ethanol treatment ($P < 0.05$).
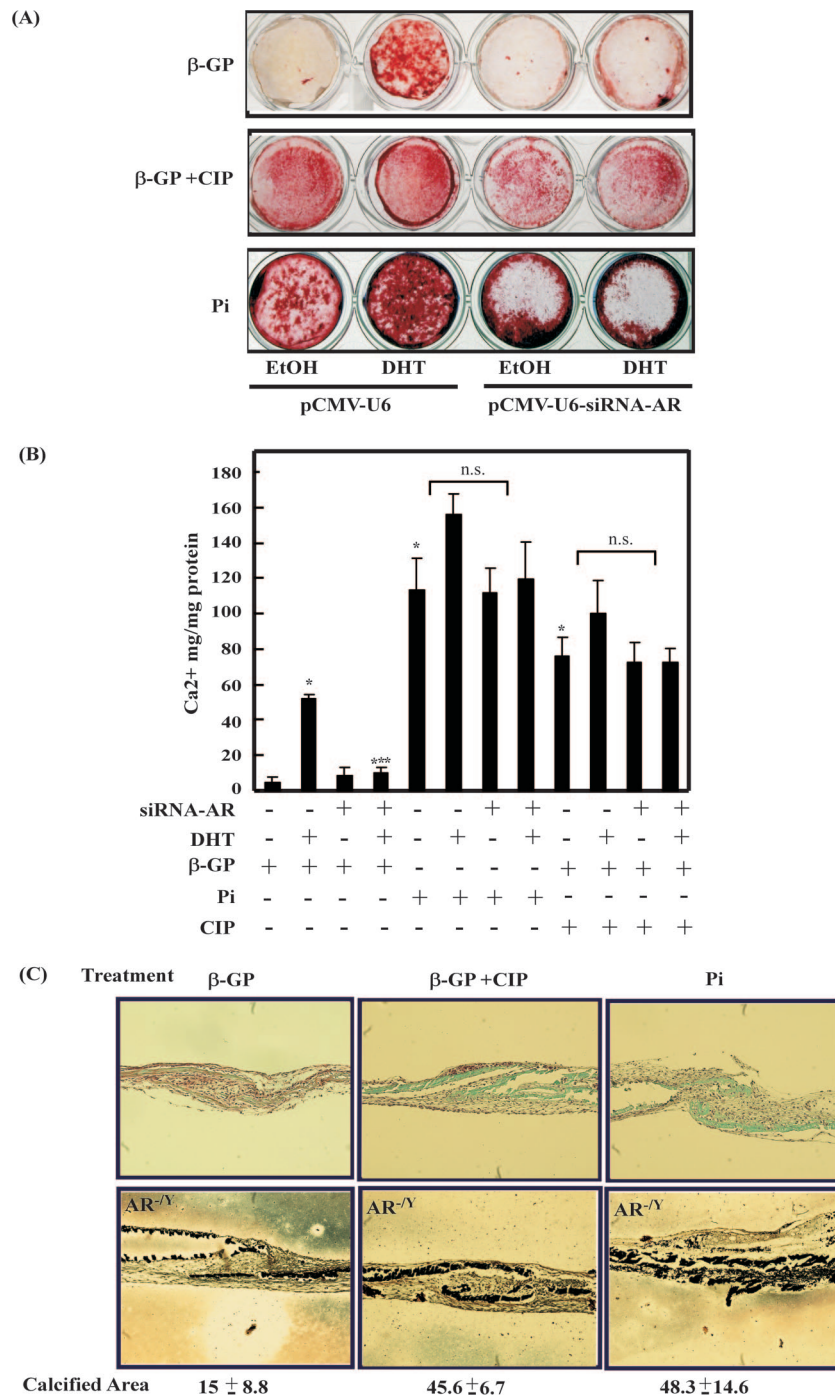
FIG. 6. TNSALP and P_i are required for AR-mediated bone mineralization. MC3T3-E1 cells stably transfected with siRNA-control (pCMV-U6) or siRNA-AR were stimulated in the absence or presence of DHT in osteogenic medium containing β-GP, β-GP+CIP, or P_i for 20 days. (A) Cells were fixed and stained with alizarin red S to assess matrix mineralization. (B) Calcium levels were determined by using the calcium deposition assay with colorimetric quantification. The data are representative of at least three independent experiments and error bars represent ± the SD. *, Samples significantly different from ethanol treatment ($P < 0.05$); ***, samples significantly different from parent vector control ($P < 0.05$). (C) Ex vivo primary calvarial bones from 3-day-old male $AR^{-/Y}$ mice were cultured with β-GP, β-GP+CIP, or P_i. The bones were then sectioned and paraffin embedded, and the areas of mineralized bone were stained with Goldner's trichrome (upper panel) and von Kossa (lower panel) staining. The values below the figures represent the calcified areas of the bone sections.

Binding to specific DNA sequences located near or within androgen target gene promoter and enhancer sequences, known as AREs and androgen regulatory regions, allows AR to facilitate interactions with the general transcriptional ma-chinery, leading to gene transcription and downstream biolog-ical effects (27). Androgen/AR also regulate gene expression by interacting with coregulators (17, 28) and nongenomic mechanisms (24). Alternatively, androgen target genes may be

regulated indirectly as a secondary or tertiary event through initial direct upregulation or liberation of transcription factors that in turn regulate the expression of other target genes (37). Such a network allows for layers of regulatory control that may be advantageous for the temporal direction of protein synthesis, the amplification of androgen signals, and the coordinated expression of genes involved in differentiation and mineralization processes.

We also identified members of the SIBLING gene family, known to bind strongly to hydroxyapatite, as androgen target genes. The regulation of SIBLING gene expression by androgens and AR may provide sufficient matrix proteins that are available at the outer membrane surface of osteoblasts and matrix vesicles for initiation of hydroxyapatite crystal formation during androgen-mediated mineralization. Previous data has shown that the entire SIBLING protein family is the result of duplication and subsequent divergent evolution of a single ancient gene (11). This finding is supported by the presence of consensus AREs in the promoter region of all members of the SIBLING gene family and the regulation of these genes by androgens/AR. The regulation of *BSP*, *DMP1*, and related SIBLING glycoprotein genes by AR is further supported by the expression of these genes in AR-positive Sertoli cells in developing testis cords (56). The presence of several different RGD-containing SIBLING gene family proteins with similar structural and biochemical properties in the ECM of bone may provide functional diversity in the promotion of mineralization. It is possible that the complement of SIBLING family proteins regulated by androgens/AR in osteoblasts may amplify the ECM-associated signals to facilitate the androgen-mediated mineralization.

While P_i generated by ALP promotes AR expression and alters its cellular localization, the molecular mechanisms are currently undefined. The ability of the phosphate transport inhibitor PFA to block phosphate-induced AR expression suggests that phosphate must enter the cell to alter cell function and supports the idea that P_i represents a novel and important intracellular signaling molecule in osteoblast differentiation. Upon entering the cell, P_i, in addition to regulating AR, has been demonstrated to alter the cellular localization of the important osteoblast transcription factor Cbfa1 (14) and to cause cell proliferation in osteoblasts through an insulinlike growth factor-1-dependent mechanism (23). Previous studies showed that phosphorylation of extracellular signal-regulated kinase (ERK1/2) and protein kinase C are specifically required for osteopontin expression in response to elevated P_i (3). In addition, it has been demonstrated that proteasomal activity is required in the phosphate-signaling pathway (3). It is well documented that AR is regulated by the ERK1/2 and proteasomal pathways in response to various stimuli (27). Therefore, it is possible that P_i may activate the ERK1/2 signaling pathway for AR expression and alters its cellular localization to modulate AR by the proteasomal pathway. Future studies will be required to provide more insights into the regulation of AR and to identify key signaling cascades initiated by an increase in intracellular P_i.

Numerous factors, including transforming growth factor β, retinoic acid, endothelin, bone morphogenic protein, and vitamin D, are known to stimulate OPN/SPP1 expression in osteoblasts (8) and to induce TNSALP and, presumably, elevate phosphate levels. Therefore, it is likely that the phosphate signal for the induction of TNSALP and OPN/SPP1 expression is a feature shared by many factors, including AR. The present study provides evidence to link the induction of AR with an increase in TNSALP activity, which in turn elevates the level of P_i to upregulate the level of AR. This mechanism provides an explanation of the specific regulation of AR in bone, since P_i does not stimulate AR expression in prostate cancer LNCaP cells (data not shown). Although the precise molecular mechanisms underlying the tissue-specific P_i-induced upregulation of AR expression remains to be elucidated, it appears not to be the result of an increase in basal protein levels.

Several reports show that global ARKO or osteoblastic-specific ARKO male mice develop osteopenia, resulting in definitive bone loss in conjunction with changes in histological analysis and increased matrix apposition rate of tibia and femur bone sections, but show but no mineralization defect (31, 38, 53, 60). In contrast, our results showed a dramatic decrease in the area of calcification, new bone, and the number of osteocytes in calvaria from ARKO mice. The discrepancy of these results may be due to the difference between endochondral and intramembranous bone development. A key feature of the mineralization of endochondral long bones is the coordination of chondrogenesis and ossification in the epiphyseal growth plate and osteogenesis in the perichondrium/periosteum. In contrast, the intramembranous bone mineralization is regulated at the suture by interactions between the mesenchyme, the osteogenic front, and the duramater, a tough, fibrous membrane forming the outer envelope of the brain and the inner lining of cranial bones and sutures (40). It is possible that the androgen/AR actions may occur at the suture for the regulation of intramembranous ossification different from endochondral ossification.

Our knowledge of sex hormone signaling pathways has advanced significantly due to the recent recognition that AR is a major mediator of androgen action in bone. The findings presented here highlight the potential of AR-deficient mice as a unique model for mineralization disorders. Given the significant therapeutic potential of lowering physiological AR levels, further investigation is essential to determine whether the role of AR in bone mineralization is conserved between mice and humans. Human genetic disorders in which abnormalities in bone development are associated with aberrations in AR imply conservation of the role of AR in bone mineralization between mice and humans. For example, hypogonadism in men is associated with an increase in bone turnover and bone loss (13, 45). Furthermore, inactivation of AR in humans results in androgen-insensitive syndromes associated with osteopenia (47). Likewise, testicular feminized mice with mutations in AR present with a phenotype consistent with that observed in humans (51). Conservation of the mechanisms underlying bone mineralization opens the potential to increase our understanding of the impact of hormonal variations on bone development and, consequently, enhance our management of ECM mineralization in humans with AR-associated bone diseases.

REFERENCES

1. **Abu, E. O., A. Horner, V. Kusec, J. T. Triffitt, and J. E. Compston.** 1997. The localization of androgen receptors in human bone. J. Clin. Endocrinol. Metab. **82:**3493–3497.

2. **Balkan, W., K. L. Burnstein, P. C. Schiller, C. Perez-Stable, G. D'Ippolito, G. A. Howard, and B. A. Roos.** 2005. Androgen-induced mineralization by MC3T3-E1 osteoblastic cells reveals a critical window of hormone responsiveness. Biochem. Biophys. Res. Commun. **328:**783–789.

3. **Beck, G. R., Jr., and N. Knecht.** 2003. Osteopontin regulation by inorganic phosphate is ERK1/2-, protein kinase C-, and proteasome-dependent. J. Biol. Chem. **278:**41921–41929.

4. **Beck, G. R., Jr., B. Zerler, and E. Moran.** 2000. Phosphate is a specific signal for induction of osteopontin gene expression. Proc. Natl. Acad. Sci. USA **97:**8352–8357.

5. **Castelo-Branco, C., J. J. Vicente, F. Figueras, A. Sanjuan, M. J. Martinez de Osaba, E. Casals, F. Pons, J. Balasch, and J. A. Vanrell.** 2000. Comparative effects of estrogens plus androgens and tibolone on bone, lipid pattern and sexuality in postmenopausal women. Maturitas **34:**161–168.

6. **Choi, J. Y., B. H. Lee, K. B. Song, R. W. Park, I. S. Kim, K. Y. Sohn, J. S. Jo, and H. M. Ryoo.** 1996. Expression patterns of bone-related proteins during osteoblastic differentiation in MC3T3-E1 cells. J. Cell Biochem. **61:**609–618.

7. **Czerwiec, F. S., J. J. Liaw, S. B. Liu, C. Perez-Stable, R. Grumbles, G. A. Howard, B. A. Roos, and K. L. Burnstein.** 1997. Absence of androgen-mediated transcriptional effects in osteoblastic cells despite presence of androgen receptors. Bone **21:**49–56.

8. **Denhardt, D. T., and M. Noda.** 1998. Osteopontin expression and function: role in bone remodeling. J. Cell Biochem. Suppl. **31:**92–102.

9. **Eaton, R. H., and D. W. Moss.** 1968. Kinetic studies on the orthophosphatase and iorganic pyrophosphatase activities of human alkaline phosphatase. Enzymologia **35:**168–178.

10. **Fedde, K. N., L. Blair, J. Silverstein, S. P. Coburn, L. M. Ryan, R. S. Weinstein, K. Waymire, S. Narisawa, J. L. Millan, G. R. MacGregor, and M. P. Whyte.** 1999. Alkaline phosphatase knockout mice recapitulate the metabolic and skeletal defects of infantile hypophosphatasia. J. Bone Miner. Res. **14:**2015–2026.

11. **Fisher, L. W., D. A. Torchia, B. Fohr, M. F. Young, and N. S. Fedarko.** 2001. Flexible structures of SIBLING proteins, bone sialoprotein, and osteopontin. Biochem. Biophys. Res. Commun. **280:**460–465.

12. **Forbes, A. P.** 1991. Fuller Albright. His concept of postmenopausal osteoporosis and what came of it. Clin. Orthop. Relat. Res.**:**128–141.

13. **Francis, R. M., M. Peacock, J. E. Aaron, P. L. Selby, G. A. Taylor, J. Thompson, D. H. Marshall, and A. Horsman.** 1986. Osteoporosis in hypogonadal men: role of decreased plasma 1,25-dihydroxyvitamin D, calcium malabsorption, and low bone formation. Bone **7:**261–268.

14. **Fujita, T., N. Izumo, R. Fukuyama, T. Meguro, H. Nakamuta, T. Kohno, and M. Koida.** 2001. Phosphate provides an extracellular signal that drives nuclear export of Runx2/Cbfa1 in bone cells. Biochem. Biophys. Res. Commun. **280:**348–352.

15. **Goulding, A., and E. Gold.** 1993. Flutamide-mediated androgen blockade evokes osteopenia in the female rat. J. Bone Miner. Res. **8:**763–769.

16. **Gruber, R., K. Czerwenka, F. Wolf, G. M. Ho, M. Willheim, and M. Peterlik.** 1999. Expression of the vitamin D receptor, of estrogen and thyroid hormone receptor alpha- and beta-isoforms, and of the androgen receptor in cultures of native mouse bone marrow and of stromal/osteoblastic cells. Bone **24:**465–473.

17. **Heinlein, C. A., and C. Chang.** 2002. Androgen receptor (AR) coregulators: an overview. Endocrinol. Rev. **23:**175–200.

18. **Henthorn, P. S., and M. P. Whyte.** 1992. Missense mutations of the tissue-nonspecific alkaline phosphatase gene in hypophosphatasia. Clin. Chem. **38:**2501–2505.

19. **Hough, T. A., M. Polewski, K. Johnson, M. Cheeseman, P. M. Nolan, L. Vizor, S. Rastan, A. Boyde, K. Pritzker, A. J. Hunter, E. M. Fisher, R. Terkeltaub, and S. D. Brown.** 2007. Novel mouse model of autosomal semidominant adult hypophosphatasia has a splice site mutation in the tissue nonspecific alkaline phosphatase gene Akp2. J. Bone Miner. Res. **22:**1397–1407.

20. **Huber, D. M., A. C. Bendixen, P. Pathrose, S. Srivastava, K. M. Dienger, N. K. Shevde, and J. W. Pike.** 2001. Androgens suppress osteoclast formation induced by RANKL and macrophage-colony stimulating factor. Endocrinology **142:**3800–3808.

21. **Ikegami, A., S. Inoue, T. Hosoi, Y. Mizuno, T. Nakamura, Y. Ouchi, and H. Orimo.** 1993. Immunohistochemical detection and northern blot analysis of estrogen receptor in osteoblastic cells. J. Bone Miner. Res. **8:**1103–1109.

22. **Johnson, K., J. Goding, D. Van Etten, A. Sali, S. I. Hu, D. Farley, H. Krug, L. Hessle, J. L. Millan, and R. Terkeltaub.** 2003. Linked deficiencies in

23. extracellular PP$_i$ and osteopontin mediate pathologic calcification associated with defective PC-1 and ANK expression. J. Bone Miner. Res. **18:**994–1004.

24. **Kanatani, M., T. Sugimoto, J. Kano, and K. Chihara.** 2002. IGF-I mediates the stimulatory effect of high phosphate concentration on osteoblastic cell proliferation. J. Cell Physiol. **190:**306–312.

25. **Kang, H. Y., C. L. Cho, K. L. Huang, J. C. Wang, Y. C. Hu, H. K. Lin, C. Chang, and K. E. Huang.** 2004. Nongenomic androgen activation of phosphatidylinositol 3-kinase/Akt signaling pathway in MC3T3-E1 osteoblasts. J. Bone Miner. Res. **19:**1181–1190.

26. **Kang, H. Y., K. E. Huang, S. Y. Chang, W. L. Ma, W. J. Lin, and C. Chang.** 2002. Differential modulation of androgen receptor-mediated transactivation by Smad3 and tumor suppressor Smad4. J. Biol. Chem. **277:**43749–43756.

27. **Kang, H. Y., H. K. Lin, Y. C. Hu, S. Yeh, K. E. Huang, and C. Chang.** 2001. From transforming growth factor-beta signaling to androgen action: identification of Smad3 as an androgen receptor coregulator in prostate cancer cells. Proc. Natl. Acad. Sci. USA **98:**3018–3023.

28. **Kang, H. Y., M. Y. Tsai, C. Chang, and K. E. Huang.** 2003. Mechanisms and clinical relevance of androgens and androgen receptor actions. Chang Gung Med. J. **26:**388–402.

29. **Kang, H. Y., S. Yeh, N. Fujimoto, and C. Chang.** 1999. Cloning and characterization of human prostate coactivator ARA54, a novel protein that associates with the androgen receptor. J. Biol. Chem. **274:**8570–8576.

30. **Kang, Z., O. A. Janne, and J. J. Palvimo.** 2004. Coregulator recruitment and histone modifications in transcriptional regulation by the androgen receptor. Mol. Endocrinol. **18:**2633–2648.

31. **Kasperk, C., A. Helmboldt, I. Borcsok, S. Heuthe, O. Cloos, F. Niethard, and R. Ziegler.** 1997. Skeletal site-dependent expression of the androgen receptor in human osteoblastic cell populations. Calcif. Tissue Int. **61:**464–473.

32. **Kawano, H., T. Sato, T. Yamada, T. Matsumoto, K. Sekine, T. Watanabe, T. Nakamura, T. Fukuda, K. Yoshimura, T. Yoshizawa, K. Aihara, Y. Yamamoto, Y. Nakamichi, D. Metzger, P. Chambon, K. Nakamura, H. Kawaguchi, and S. Kato.** 2003. Suppressive function of androgen receptor in bone resorption. Proc. Natl. Acad. Sci. USA **100:**9416–9421.

33. **Manolagas, S. C., S. Kousteni, and R. L. Jilka.** 2002. Sex steroids and bone. Recent Prog. Horm. Res. **57:**385–409.

34. **Mizuno, Y., T. Hosoi, S. Inoue, A. Ikegami, M. Kaneki, Y. Akedo, T. Nakamura, Y. Ouchi, C. Chang, and H. Orimo.** 1994. Immunocytochemical identification of androgen receptor in mouse osteoclast-like multinucleated cells. Calcif. Tissue Int. **54:**325–326.

35. **Mundy, G., R. Garrett, S. Harris, J. Chan, D. Chen, G. Rossini, B. Boyce, M. Zhao, and G. Gutierrez.** 1999. Stimulation of bone formation in vitro and in rodents by statins. Science **286:**1946–1949.

36. **Murshed, M., D. Harmey, J. L. Millan, M. D. McKee, and G. Karsenty.** 2005. Unique coexpression in osteoblasts of broadly expressed genes accounts for the spatial restriction of ECM mineralization to bone. Genes Dev. **19:**1093–1104.

37. **Nakano, Y., I. Morimoto, O. Ishida, T. Fujihira, A. Mizokami, A. Tanimoto, N. Yanagihara, F. Izumi, and S. Eto.** 1994. The receptor, metabolism and effects of androgen in osteoblastic MC3T3-E1 cells. Bone Miner. **26:**245–259.

38. **Nelson, P. S., N. Clegg, H. Arnold, C. Ferguson, M. Bonham, J. White, L. Hood, and B. Lin.** 2002. The program of androgen-responsive genes in neoplastic prostate epithelium. Proc. Natl. Acad. Sci. USA **99:**11890–11895.

39. **Notini, A. J., J. F. McManus, A. Moore, M. Bouxsein, M. Jimenez, W. S. Chiu, V. Glatt, B. E. Kream, D. J. Handelsman, H. A. Morris, J. D. Zajac, and R. A. Davey.** 2007. Osteoblast deletion of exon 3 of the androgen receptor gene results in trabecular bone loss in adult male mice. J. Bone Miner. Res. **22:**347–356.

40. **Orimo, H., and T. Shimada.** 2005. Regulation of the human tissue-nonspecific alkaline phosphatase gene expression by all-trans-retinoic acid in SaOS-2 osteosarcoma cell line. Bone **36:**866–876.

41. **Ornitz, D. M., and P. J. Marie.** 2002. FGF signaling pathways in endochondral and intramembranous bone development and human genetic disease. Genes Dev. **16:**1446–1465.

42. **Parfitt, A. M., M. K. Drezner, F. H. Glorieux, J. A. Kanis, H. Malluche, P. J. Meunier, S. M. Ott, R. R. Recker, et al.** 1987. Bone histomorphometry: standardization of nomenclature, symbols, and units. J. Bone Miner. Res. **2:**595–610.

43. **Pederson, L., M. Kremer, J. Judd, D. Pascoe, T. C. Spelsberg, B. L. Riggs, and M. J. Oursler.** 1999. Androgens regulate bone resorption activity of isolated osteoclasts in vitro. Proc. Natl. Acad. Sci. USA **96:**505–510.

44. **Rao, L. G., J. N. Wylie, M. S. Kung Sutherland, and T. M. Murray.** 1996. 17β-Oestradiol enhances the stimulatory effect of 1,25-dihydroxyvitamin D$_3$ on alkaline phosphatase activity in human osteosarcoma SaOS-2 cells in a differentiation-dependent manner. J. Endocrinol. **148:**181–187.

45. **Reifenstein, E. C., and F. Albright.** 1947. The metabolic effects of steroid hormones in osteoporosis. J. Clin. Investig. **26:**24–56.

46. **Rochira, V., A. Balestrieri, B. Madeo, L. Zirilli, A. R. Granata, and C. Carani.** 2006. Osteoporosis and male age-related hypogonadism: role of sex steroids on bone (patho)physiology. Eur. J. Endocrinol. **154:**175–185.

47. **Sato, T., H. Kawano, and S. Kato.** 2002. Study of androgen action in bone by

analysis of androgen-receptor deficient mice. J. Bone Miner. Metab. **20:**326–330.

47. **Soule, S. G., G. Conway, G. M. Prelevic, M. Prentice, J. Ginsburg, and H. S. Jacobs.** 1995. Osteopenia as a feature of the androgen insensitivity syndrome. Clin. Endocrinol. **43:**671–675.

48. **Takeuchi, M., H. Kakushi, and M. Tohkin.** 1994. Androgens directly stimulate mineralization and increase androgen receptors in human osteoblast-like osteosarcoma cells. Biochem. Biophys. Res. Commun. **204:**905–911.

49. **Teitelbaum, S. L.** 2000. Bone resorption by osteoclasts. Science **289:**1504–1508.

50. **Traianedes, K., M. R. Dallas, I. R. Garrett, G. R. Mundy, and L. F. Bonewald.** 1998. 5-Lipoxygenase metabolites inhibit bone formation in vitro. Endocrinology **139:**3178–3184.

51. **Vandenput, L., J. V. Swinnen, S. Boonen, E. Van Herck, R. G. Erben, R. Bouillon, and D. Vanderschueren.** 2004. Role of the androgen receptor in skeletal homeostasis: the androgen-resistant testicular feminized male mouse model. J. Bone Miner. Res. **19:**1462–1470.

52. **Vanderschueren, D., L. Vandenput, S. Boonen, M. K. Lindberg, R. Bouillon, and C. Ohlsson.** 2004. Androgens and bone. Endocrinol. Rev. **25:**389–425.

53. **Venken, K., K. De Gendt, S. Boonen, J. Ophoff, R. Bouillon, J. V. Swinnen, G. Verhoeven, and D. Vanderschueren.** 2006. Relative impact of androgen and estrogen receptor activation in the effects of androgens on trabecular and cortical bone in growing male mice: a study in the androgen receptor knockout mouse model. J. Bone Miner. Res. **21:**576–585.

54. **Waymire, K. G., J. D. Mahuren, J. M. Jaje, T. R. Guilarte, S. P. Coburn, and G. R. MacGregor.** 1995. Mice lacking tissue nonspecific alkaline phosphatase die from seizures due to defective metabolism of vitamin B_6. Nat. Genet. **11:**45–51.

55. **Whyte, M. P.** 1994. Hypophosphatasia and the role of alkaline phosphatase in skeletal mineralization. Endocrinol. Rev. **15:**439–461.

56. **Wilson, M. J., L. Liaw, and P. Koopman.** 2005. Osteopontin and related SIBLING glycoprotein genes are expressed by Sertoli cells during mouse testis development. Dev. Dyn. **233:**1488–1495.

57. **Wiren, K., E. Keenan, X. Zhang, B. Ramsey, and E. Orwoll.** 1999. Homologous androgen receptor up-regulation in osteoblastic cells may be associated with enhanced functional androgen responsiveness. Endocrinology **140:**3114–3124.

58. **Wiren, K. M., X. Zhang, C. Chang, E. Keenan, and E. S. Orwoll.** 1997. Transcriptional up-regulation of the human androgen receptor by androgen in bone cells. Endocrinology **138:**2291–2300.

59. **Wiren, K. M., X. W. Zhang, A. R. Toombs, V. Kasparcova, M. A. Gentile, S. Harada, and K. J. Jepsen.** 2004. Targeted overexpression of androgen receptor in osteoblasts: unexpected complex bone phenotype in growing animals. Endocrinology **145:**3507–3522.

60. **Yeh, S., M. Y. Tsai, Q. Xu, X. M. Mu, H. Lardy, K. E. Huang, H. Lin, S. D. Yeh, S. Altuwaijri, X. Zhou, L. Xing, B. F. Boyce, M. C. Hung, S. Zhang, L. Gan, and C. Chang.** 2002. Generation and characterization of androgen receptor knockout (ARKO) mice: an in vivo model for the study of androgen functions in selective tissues. Proc. Natl. Acad. Sci. USA **99:**13498–13503.